



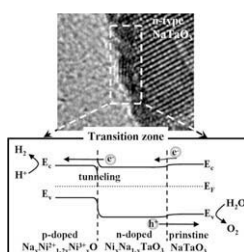
Journal of Catalysis Vol. 272, Issue 1, 2010

Contents

Structural features of p-type semiconducting NiO as a co-catalyst for photocatalytic water splitting

pp 1–8

Che-Chia Hu, Hsisheng Teng*

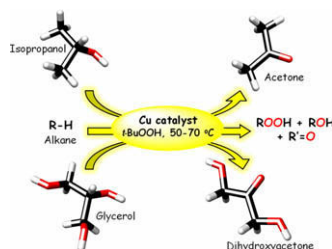


The interdiffusion of Ni^{2+} and Na^+ can form p-doped NiO (i.e. $\text{Na}_x\text{Ni}_{1-2x}\text{Ni}^{2+}\text{Ni}_x^{3+}\text{O}$) and n-doped NaTaO_3 (i.e. $\text{Ni}_x\text{Na}_{1-x}\text{TaO}_3$) at the interface and facilitate charge transport for splitting water.

Mild homogeneous oxidation of alkanes and alcohols including glycerol with *tert*-butyl hydroperoxide catalyzed by a tetracopper(II) complex

pp 9–17

Marina V. Kirillova, Alexander M. Kirillov*, Dalmo Mandelli**, Wagner A. Carvalho, Armando J.L. Pombeiro, Georgiy B. Shul'pin

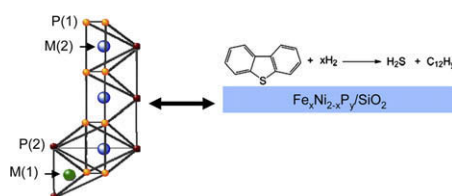


The combination of hydrosoluble tetracopper(II) catalyst with *tert*-butyl hydroperoxide leads to a versatile homogeneous system for the oxidative functionalization, under mild conditions, of various substrates that include alkanes, alcohols and glycerol.

Mössbauer spectroscopy investigation and hydrodesulfurization properties of iron–nickel phosphide catalysts

pp 18–27

Amy F. Gaudette, Autumn W. Burns, John R. Hayes, Mica C. Smith, Richard H. Bowker, Takele Seda, Mark E. Bussell*

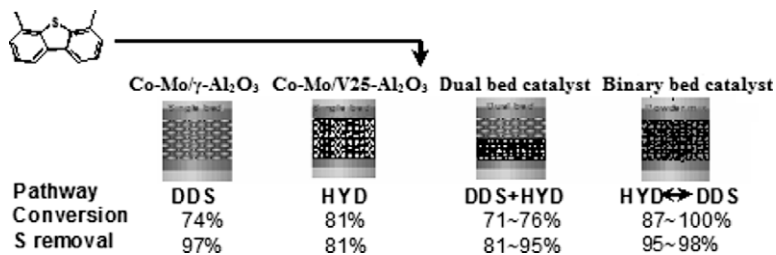


Mössbauer spectroscopy was used to determine that metal atoms are preferentially ordered in $\text{Fe}_x\text{Ni}_{2-x}\text{P}_y/\text{SiO}_2$ catalysts. The high hydrodesulfurization activity of Ni-rich $\text{Fe}_x\text{Ni}_{2-x}\text{P}_y/\text{SiO}_2$ catalysts is attributed to Ni atoms in M(2) sites at the surface of the phosphide particles.

Promoter effect of vanadia on Co/Mo/Al₂O₃ catalyst for deep hydrodesulfurization via the hydrogenation reaction pathway

pp 28–36

Ting-Mu Chen, Chih-Ming Wang, Ikai Wang, Tseng-Chang Tsai*

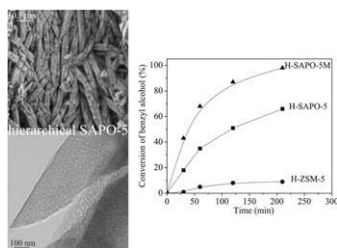


The binary catalyst system Co-Mo/γ-Al₂O₃||Co-Mo/V_x-Al₂O₃ showed high conversion of refractory sulfur compounds by concerted hydrogenation and direct desulfurization.

Hierarchical SAPO-5 catalysts active in acid-catalyzed reactions

pp 37–43

Nadiya Danilina, Frank Krumeich, Jeroen A. van Bokhoven*

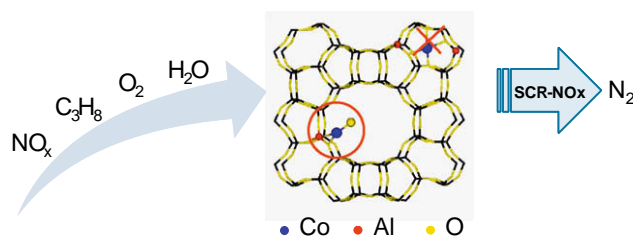


Hierarchical SAPO-5 was synthesized using a soft template with a silicon containing head-group. Its catalytic activity was much higher in space-demanding alkylation compared to the microporous analogue and H-ZSM-5.

The decisive role of the distribution of Al in the framework of beta zeolites on the structure and activity of Co ion species in propane-SCR-NO_x in the presence of water vapour

pp 44–54

L. Čapek, J. Dědeček, P. Sazama, B. Wichterlová*

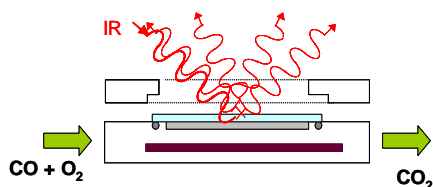


Al distribution in the framework controls the structure and activity of Co species in Co-BEA zeolites. Co-oxo species balanced by Al_{isol} are highly active in C₃H₈-SCR-NO_x at 10% H₂O.

Spatially resolved catalysis in microstructured reactors by IR spectroscopy: CO oxidation over mono- and bifunctional Pt catalysts

pp 55–64

C. Daniel, M-O. Clarté, S.-P. Teh, O. Thinon, H. Provendier, A.C. Van Veen, B.J. Beccard, Y. Schuurman*, C. Mirodatos

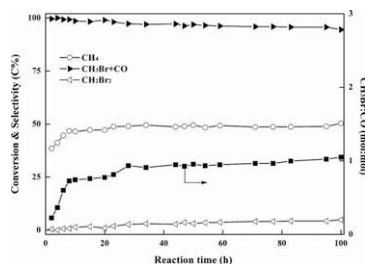


CO oxidation has been studied in a new microstructured DRIFTS cell over platinum catalysts. Modeling of the data shows that addition of ceria changes the rate-controlling step.

Efficient and stable silica-supported iron phosphate catalysts for oxidative bromination of methane

pp 65–73

Ronghe Lin, Yunjie Ding*, Leifeng Gong, Wenda Dong, Junhu Wang, Tao Zhang**

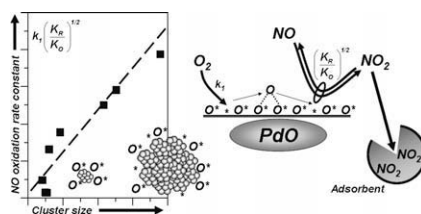


Oxidative bromination of methane over FePO₄/SiO₂ catalyst was dominated by a redox route, which gave 50% methane conversion and 96% total selectivity toward CH₃Br/CO (CH₃Br:CO ≈ 1) at 570 °C.

Mechanism and site requirements for NO oxidation on Pd catalysts

pp 74–81

Brian M. Weiss, Enrique Iglesia*

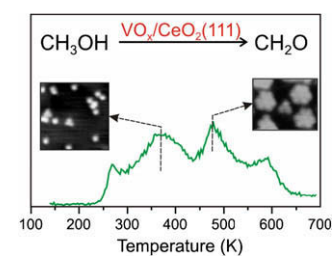


O₂ activation on scarce vacancy sites in PdO clusters limits NO oxidation rates. The kinetic relevance of these vacancies causes turnover rates to increase as oxygen binding weakens with increasing cluster size and as adsorbents deplete NO₂ near active sites.

Relating methanol oxidation to the structure of ceria-supported vanadia monolayer catalysts

pp 82–91

H.L. Abbott*, A. Uhl, M. Baron, Y. Lei, R.J. Meyer, D.J. Stacchiola, O. Bondarchuk, S. Shaikhutdinov**, H.J. Freund

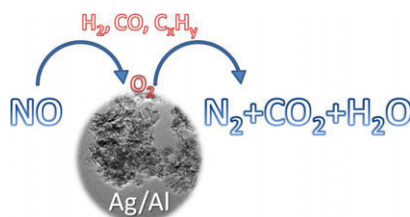


Methanol oxidation to formaldehyde was studied on well-defined VO_x/CeO₂ model catalysts as a function of vanadia coverage. The results revealed a low temperature reaction pathway, which is assigned to isolated vanadyl species surrounded by a reduced ceria surface.

Sol-gel-entrapped nano silver catalysts-correlation between active silver species and catalytic behavior

pp 92–100

Vasile I. Pârvulescu*, Bogdan Cojocaru, Viorica Pârvulescu, Ryan Richards**, Zhi Li, Chris Cadigan, Pascal Granger***, Pierre Miquel, Chris Hardacre****

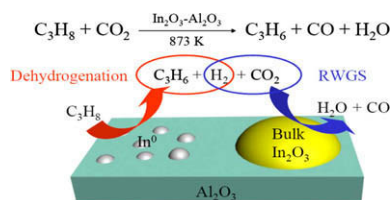


The target reaction is the reduction of NO to nitrogen which competes with the oxidation reaction under lean conditions (excess of oxygen) that may considerably alter the selectivity. Silver colloids prepared by reducing AgNO₃ in aqueous solution are embedded in alumina leading to stable nano-catalysts. The activity of the catalysts is influenced by the preparation procedure.

Dehydrogenation of propane over $\text{In}_2\text{O}_3\text{-Al}_2\text{O}_3$ mixed oxide in the presence of carbon dioxide

pp 101–108

Miao Chen, Jie Xu, Yong Cao*, He-Yong He, Kang-Nian Fan, Ji-Hua Zhuang**

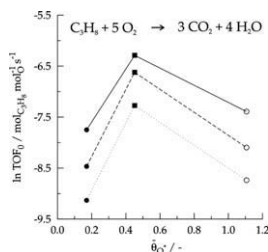


$\text{In}_2\text{O}_3\text{-Al}_2\text{O}_3$ mixed oxides were found to be active and stable for propane dehydrogenation with CO_2 , in which a unique bifunctional character of the indium component has been established.

The total oxidation of propane over supported Cu and Ce oxides: A comparison of single and binary metal oxides

pp 109–120

Philippe M. Heynderickx, Joris W. Thybaut*, Hilde Poelman, Dirk Poelman, Guy B. Marin

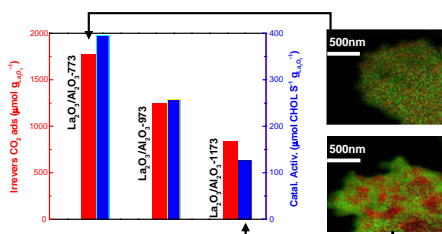


The reduction and reoxidation characteristics of single metal oxides, $\text{CuO}/\theta\text{-Al}_2\text{O}_3$ (○) and $\text{CeO}_2/\gamma\text{-Al}_2\text{O}_3$ (●), are combined in a synergistic way: initial turnover frequencies are highest on the binary metal oxide catalyst, $\text{CuO-CeO}_2/\gamma\text{-Al}_2\text{O}_3$ (■).

Influence of the calcination temperature on the nano-structural properties, surface basicity, and catalytic behavior of alumina-supported lanthana samples

pp 121–130

Zouhair Boukha, Loubna Fitian, Miguel López-Haro, Manuel Mora, José Rafael Ruiz, César Jiménez-Sanchidrián, Ginesa Blanco, José J. Calvino, Gustavo A. Cifredo, Susana Trasobares, Serafín Bernal*

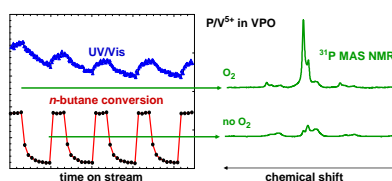


The influence of the calcination temperature on the lanthana distribution, surface basicity, and catalytic properties of a $\text{La}_2\text{O}_3/\text{Al}_2\text{O}_3$ sample, with lanthana loading close to the theoretical monolayer, is discussed. The resulting materials represent an advantageous alternative to pure lanthana as highly basic catalysts.

Quantitative solid-state NMR investigation of V^{5+} species in VPO catalysts upon sequential selective oxidation of *n*-butane

pp 131–139

Jörg Frey, Christian Lieder, Thomas Schölkopf, Thomas Schleid, Ulrich Nieken, Elias Klemm, Michael Hunger*

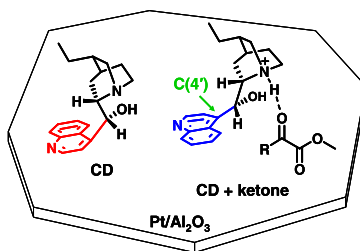


Assignment and quantification of active V^{5+} species of VPO catalysts applied for the selective oxidation of *n*-butane to maleic anhydride were performed by *on-line* UV/Vis and ^{31}P MAS NMR spectroscopy.

Substrate-controlled adsorption of cinchonidine during enantioselective hydrogenation on platinum

pp 140–150

Erik Schmidt, Tamas Mallat, Alfons Baiker*

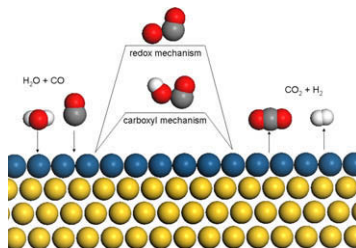


The dominant adsorption mode of cinchonidine on Pt/Al₂O₃ inverts from pro-(S) at C(4') to pro-(R) upon interaction with the ketone substrate, as concluded from the product distribution of the hydrogenation of its anchoring quinoline ring.

A density functional theory study of water gas shift over pseudomorphic monolayer alloy catalysts: Comparison with NO oxidation

pp 151–157

Jelena Jelic, Randall J. Meyer*

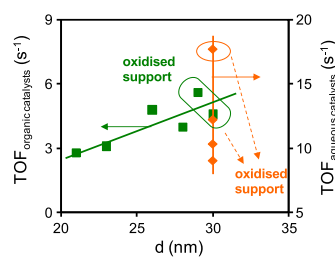


The carboxyl mechanism was found to be favored for water gas shift over Pt-based pseudomorphic monolayer systems.

Carbon nanofibre-supported palladium catalysts as model hydrodechlorination catalysts

pp 158–168

Salvador Ordóñez*, Eva Díaz, Rubén F. Bueres, Esther Asedegbega-Nieto, Herminio Sastre

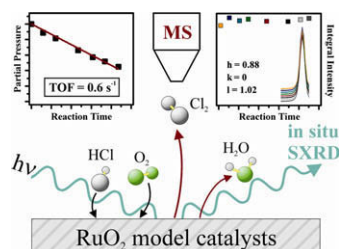


The activity and deactivation of different CNF-supported palladium catalysts (using different precursors and surface treatments) for tetrachloroethylene hydrodechlorination have been studied in this work. It was observed that the behaviour of the catalysts changes markedly with the treatment of the surface and, more markedly, with the impregnation procedure (using organic or aqueous solutions). Characterisation of the fresh and aged samples by different techniques allows to explain this behaviour.

In situ studies of the oxidation of HCl over RuO₂ model catalysts: Stability and reactivity

pp 169–175

S. Zweidinger, J.P. Hofmann, O. Balmes, E. Lundgren, H. Over*

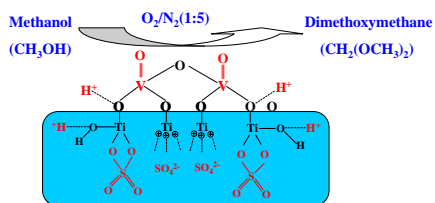


In situ surface X-ray diffraction reveals that RuO₂-model catalysts are long-term stable for the HCl oxidation reaction by oxygen with a mean TOF of 0.6 s⁻¹ for Cl₂ using a batch reactor.

Nature of surface sites of V_2O_5 – TiO_2/SO_4^{2-} catalysts and reactivity in selective oxidation of methanol to dimethoxymethane

pp 176–189

Hongying Zhao, Simona Bennici, Jianyi Shen, Aline Auroux*



Catalytic activity of sulfated vanadia–titania catalysts measured in selective methanol oxidation to dimethoxymethane was found to depend on the nature of surface sites, calcination temperature, and sulfate concentration.